The periodogram and Allan variance reveal fractal exponents greater than unity in auditory-nerve spike trains

Steven B. Lowen
Department of Electrical Engineering, 500 West 120th Street, Columbia University, New York, New York 10027

Malvin C. Teich
Department of Electrical and Computer Engineering, and Hearing Research Center, Department of Biomedical Engineering, Boston University, 44 Cummington Street, Boston, Massachusetts 02215

(Received 25 August 1995; accepted for publication 25 January 1996)

Auditory-nerve spike trains exhibit fractal behavior, and therefore traditional renewal-point-process models fail to describe them adequately. Previous measures of the fractal exponent of these spike trains are based on the Fano factor and consequently cannot exceed unity. Two estimates of the fractal exponent are considered which do not suffer from this limit: one derived from the Allan variance, which was developed by the authors, and one based on the periodogram. These measures indicate that fractal exponents do indeed exceed unity for some nerve-spike recordings from stimulated primary afferent cat auditory-nerve fibers. © *1996 Acoustical Society of America.*

PACS numbers: 43.64.Pg, 43.64.Bt

INTRODUCTION

The mathematical model that has been traditionally used in auditory and other branches of sensory neurophysiology is the homogeneous Poisson point process (HPP) and its close relatives, the family of refractoriness-modified Poisson point processes (RMPs). Members of this family include processes with refractoriness that is fixed (Ricciardi and Esposito, 1966), random with a Gaussian distribution (Teich *et al.*, 1978), random with an exponential distribution (Young and Barta, 1986), and a combination of the first and last kinds (Li and Young, 1993). All of these processes are renewal, which means that they exhibit independent, identically distributed interevent intervals. These intervals are therefore uncorrelated, and such processes are completely specified by their interevent-interval histograms (IIHs).

Figure 1 displays the IIH for the spontaneous neural activity observed on a typical primary afferent (VIII-nerve) cat auditory-nerve fiber. This particular neuron has a characteristic frequency (CF) of 3926 Hz. The approximately straight-line behavior of the data for interevent intervals greater than about 5 ms on this semilogarithmic plot (solid curve) demonstrates that the histogram has an exponential tail. The HPP and the RMP models mentioned above (all except the Gaussian) were fit to the IIH by setting the first k moments of the theoretical density function equal to those of the data, where k is the number of parameters in each model. All three models correctly yield an exponential tail; we illustrate only the exponentially distributed random dead-time model (denoted EXP-RMP; dashed curve) since it provides a reasonably good fit to the data with a minimum of parameters. The combined fixed-and-random dead-time model (Li and Young, 1993) fits the data slightly better for this data set, but at the expense of an additional parameter. Although the RMP models fit the IIH well, they fail to accord with many other statistical features of auditory-nerve spike data. Therefore, the sequence of auditory nerve spikes is *not* renewal (Lowen and Teich, 1992), despite a long history of papers to the contrary.

I. FRACTAL BEHAVIOR IN AUDITORY-NERVE SPIKE TRAINS

Auditory-nerve spike trains exhibit correlations. Sequences of interevent intervals exhibit positive correlation over the long term (Teich, 1989) and often exhibit negative correlation over the short term (Lowen and Teich, 1992). Such spike trains are therefore not renewal, and RMP models cannot properly describe them (Teich, 1992). Rather, a description of the nerve-spike train requires a fractal-stochastic-point-process (FSPP) model (Teich, 1989; Teich, 1992; Teich *et al.*, 1990a, 1990b; Powers *et al.*, 1991; Powers and Salvi, 1992; Woo *et al.*, 1992; Kumar and Johnson, 1993; Kelly *et al.*, 1996).

A. Self-similarity of neuronal firing rates

Perhaps the simplest measure of a sequence of action potentials is its rate: the number of spikes registered per unit time. For nonfractal processes such as RMPs, fluctuations in the rate estimate tend to average out as the counting time used to compute the rate increases. In auditory neural firings this appears to occur much more slowly; even this straightforward measure has fractal properties. The fluctuations of the rate often do not decrease appreciably even when a very long counting time is used to compute the rate, but instead exhibit fluctuations on all time scales (Teich *et al.*, 1990a; Teich, 1992). This behavior derives from correlations in the sequence of interevent intervals, as confirmed by the observation that the fractal properties of the rate estimate are destroyed by shuffling (randomly reordering) the intervals. This operation removes the correlations among the intervals while exactly preserving the interevent-interval histogram. With all dependencies among the intervals eliminated by shuffling (besides those inherent in retaining the same IIH), the result is essentially a renewal point process, which the random RMP indeed models very well. All statistics of the exponentially distributed random RMP model appear to closely mimic those of the *shuffled* auditory data.

 0001-4966/96/99(6)/3585/7/$6.00

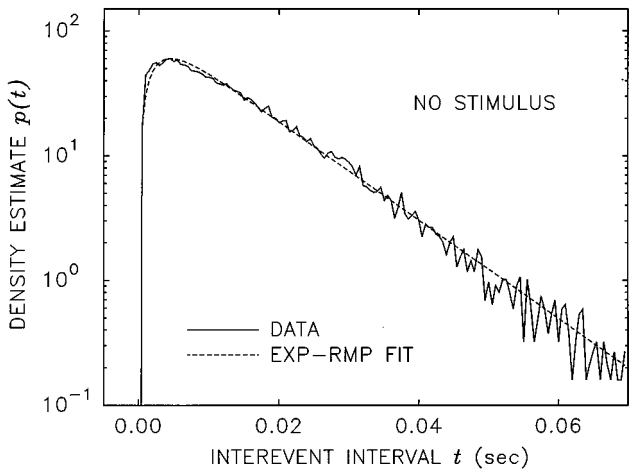

FIG. 1. Semilogarithmic plot of the relative frequency of interevent intervals for spontaneous neural activity in an auditory-nerve fiber (L-19, solid curve). The stimulus frequency at which this neuron is most sensitive (known as its characteristic frequency or CF) is 3926 Hz. The data closely follow a straight line for intervals greater than about 5 ms. Bin width is 0.5 ms. Also shown is the theoretical result for an exponentially distributed refractoriness-modified Poisson point process (EXP-RMP) with the same mean and variance (dashed curve).

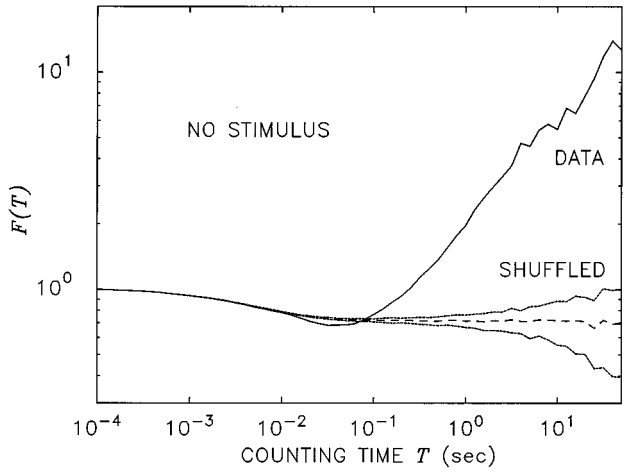

FIG. 2. Doubly logarithmic plot of the Fano factor (solid curve) for the same auditory neuron (L-19) as illustrated in Fig. 1. For counting times of about 100 ms and larger, this curve approximately follows a straight line, representing a fractional power-law increase in the Fano factor with counting time. Also shown is the FF for the shuffled data, which behaves like the FF for an RMP. The data were shuffled 100 times, and the FF computed for each set; the mean (dashed curve) $\pm$1-standard-deviation limits (dotted curves) are displayed here. The FF for the shuffled data exceeds that for the original data near $T=30$ ms, indicating that the spike train exhibits negative short-term correlation in the sequence of interevent intervals.

B. Power-law behavior of the Fano factor

Another measure sensitive to correlations is the Fano factor (FF), which is the variance of the number of neural spikes in a specified counting time T divided by the mean number of spikes in that counting time. If $N(s,t)$ is the number of spikes recorded in a counting window beginning at time s and ending at time t, then the FF $F(T)$ of a stationary data set is

$$F(T) \equiv \frac{\mathrm{E}[N^2(t,t+T)] - \mathrm{E}^2[N(t,t+T)]}{\mathrm{E}[N(t,t+T)]}, \tag{1}$$

where $\mathrm{E}[x]$ denotes the expectation of the quantity x. In general the Fano factor varies with the counting time T; hence the notation $F(T)$.

The solid curve in Fig. 2 shows the experimental FF for the same spontaneously firing neuron whose IIH is shown in Fig. 1. The Fano factor increases steadily for counting times greater than about 100 ms, and exceeds a value of ten for counting times in excess of 30 s. Since the FF approximates a straight line over a large range of counting times on this doubly logarithmic plot, it is well fit over this range by an increasing power-law function of the counting time

$$F(T) \approx 1 + (T/T_0)^{\alpha_F}, \tag{2}$$

with $\alpha_F \approx 0.48$ for this particular neuron.

Such a monotonic, power-law increase indicates the presence of fluctuations on many time scales, with the exponent α_F identified as an estimate of the fractal exponent of the point process describing this recording (Lowen and Teich, 1995a). For large counting times, all auditory-nerve spike trains examined to date in the cat, chinchilla, and chicken exhibit Fano factors that increase as power-law functions of the counting time (Teich, 1989, 1992; Teich *et al.*, 1990a, 1990b; Powers *et al.*, 1991; Powers and Salvi, 1992; Woo *et al.*, 1992; Kumar and Johnson, 1993; Kelly *et al.*, 1996). The fractal exponent α_F estimates a parameter of the spike-train recording, and serves to characterize the neuron and stimulus conditions, much as the average firing rate does. For RMP processes, the Fano factor remains near or below unity for all counting times.

A plot of the FF alone cannot reveal whether this large Fano factor arises from the distribution of the interevent intervals (the IIH), or from their ordering. This issue is resolved by plotting the Fano factor for the shuffled intervals. FFs constructed from shuffled data retain information about the relative sizes of the intervals only; all correlations and dependencies among the intervals are destroyed by the shuffling process (besides those due to the shape of the IIH), as discussed in Sec. I A. The dashed curve in Fig. 2 illustrates the FF obtained by this method. This curve behaves very much like the FF for an RMP, approaching a value less than unity for large counting times. This is consistent with the loss of self-similarity in the firing rate discussed in Sec. I A and shows that it is the ordering of the intervals, which in turn reflects correlations in the spike occurrences, that gives rise to the power-law growth of the FF for auditory neurons.

Plots of the shuffled and unshuffled FFs also highlight the small but significant negative correlation over times scales on the order of tens of ms which exists in most of the data sets we have studied ($p<2\times10^{-9}$) (Lowen and Teich, 1992; Teich and Lowen, 1994) (see also Gaumond *et al.*, 1982). This is evident in Fig. 2; an increase in the magnitude of the FF with shuffling near $T=30$ ms indicates the presence of anticorrelation in the sequence of original interevent intervals. For this particular neuron, then, long intervals are more likely to be followed by short intervals and vice versa. Many auditory neurons (but not all) behave this way (Lowen and Teich, 1992; Gaumond, 1993). Thus over the short term, as well as over the long term, neural activity on auditory-

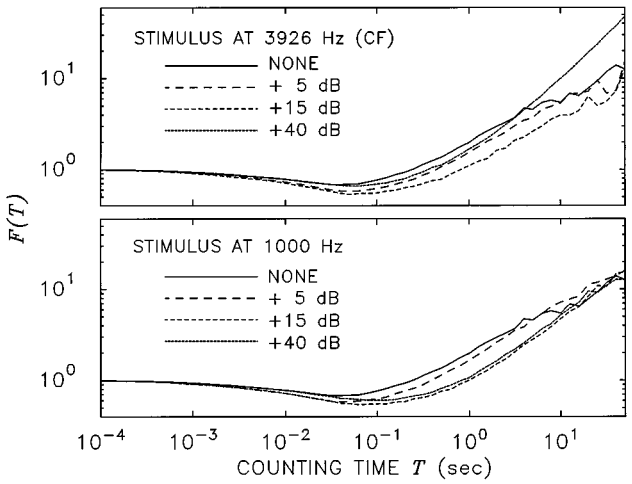

FIG. 3. Fano factors for this same neuron (L-19) when the stimulation is a continuous tone at CF (3926 Hz, upper panel) and below CF at 1000 Hz (lower panel). Stimulus levels are indicated in dB above the threshold of the neuron. The Fano factor for spontaneous firing, shown in Fig. 2, is reproduced for purposes of comparison (solid curves). The shapes of the FF curves are similar for spontaneous and driven firing; all reveal an approximately power-law increase with the counting time. The power-law exponent α_F generally increases when a stimulus is applied.

nerve fibers cannot be modeled as a renewal point process.

The FF for this same auditory neuron is shown in the upper panel of Fig. 3 when the ear is stimulated by a continuous tone at the CF, with the acoustic intensity levels (dB *re*: threshold) indicated. The spontaneous FF shown in Fig. 2 is reproduced for comparison. The lower panel of Fig. 3 presents the FFs when the frequency of the applied stimulus is 1000 Hz (below CF). Various characteristics of the neuron and stimulus are presented in Table I for this and a number of other data sets.

The FF plots shown in Fig. 3 all have a similar appearance; however, the minimum value of the Fano factor is reduced under stimulation. This occurs because the refractoriness in the neuron regularizes the spike train more effectively when the rate is higher, and thereby reduces the count variance. This effect dominates the reduction of any anticorrelation which might have existed in the interevent intervals under spontaneously firing conditions (as shown in Fig. 2). Another potential contributor is phase locking, which also reduces the count variance. The estimated Fano-factor exponent α_F also appears to increase under stimulation (Teich, 1992; Teich *et al.*, 1990a; Kelly *et al.*, 1996), although other estimation methods can give different results (Kelly, 1994; Kelly *et al.*, 1996). The FF detects the presence of self-similarity even when it cannot be discerned in visual representations of the nerve-spike train. However, it cannot increase faster than $\sim T^1$, so that the FF provides a measure of fractal exponents in the range $0<\alpha<1$ only (Lowen and Teich, 1993, 1995a; Teich *et al.*, 1996a).

C. Power-law behavior of the Allan factor and the periodogram

The accurate estimation of a fractal exponent that may assume a value greater than unity requires the use of a measure whose power-law exponent is not constrained to lie below unity. We consider two such measures.

We call the first the Allan factor (AF) (Teich *et al.*, 1996a), and define it as the ratio of the Allan variance of the event count to twice the mean. The Allan variance, in turn, represents the average variation in the difference of adjacent counts (Allan, 1966; Barnes and Allan, 1966). In terms of the numbers of counts $N(s,t)$ defined earlier, the Allan factor $A(T)$ for a stationary data set is defined as

TABLE I. Estimates of the fractal exponent employing the Fano factor (FF), the Allan factor (AF), and the periodogram (PG). All estimates were calculated by determining the slope of a least-squares straight-line fit to doubly logarithmic plots of the indicated measures. For the FF and AF, the counting time ranged from $L/100$ to $L/10$ in ten logarithmically spaced steps, where L was the duration of the recording. For the PG the frequency ranged from $1/L$ to $50/L$ in 50 linearly spaced steps. Also shown for each recording are the record name, characteristic frequency (CF) in Hz, estimate of the spontaneous rate (SR) in spikes/s, stimulus frequency in Hz, acoustic intensity in dB above threshold, and duration of the recording in seconds. Four of the recordings (L-19-6, L-19-8, R-4-4, and R-7-3) appear to have true fractal exponents greater than unity, since both the AF- and PG-based estimates exceed unity for these data files. The FF-based estimate, in contrast, cannot exceed unity.

Neuron			Stimulus			Fractal exponent estimates		
Record name	CF (Hz)	Rate est. (spikes/s)	Frequency (Hz)	Intensity (dB)	Duration (s)	α_F	α_A	α_S
L-19-3	3926	75.1	⋯	⋯	500	0.48	0.48	0.48
L-19-7	3926	93.7	3926	+5	501	0.43	0.64	0.68
L-19-5	3926	108.8	3926	+15	502	0.55	0.64	0.59
L-19-6	3926	93.8	3926	+40	502	0.96	1.11	1.27
L-19-10	3926	93.2	1000	+5	501	0.54	0.77	0.78
L-19-8	3926	103.8	1000	+15	501	0.78	1.17	1.07
L-19-9	3926	95.7	1000	+40	500	0.74	0.87	0.94
R-4-2	3342	78.8	⋯	⋯	502	0.74	0.83	0.88
R-4-4	3342	71.4	3342	+15	500	0.75	1.29	1.13
R-4-6	3342	79.1	3342	+40	350	0.80	0.85	1.39
R-7-2	281	14.1	⋯	⋯	501	0.62	0.61	0.72
R-7-3	281	93.6	281	+15	303	0.91	1.19	1.56

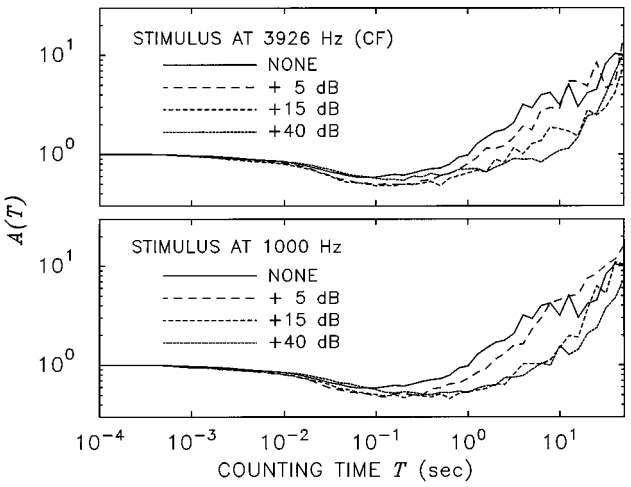

FIG. 4. Doubly logarithmic plots of the Allan factor versus counting time for the same recordings as in Fig. 3 (neuron L-19). As with the FF curves in Fig. 3, the shapes of the Allan factor plots resemble each other. All increase approximately as a power-law function of the counting time. Driven recordings yield a larger estimated fractal exponent α_A than do spontaneous recordings.

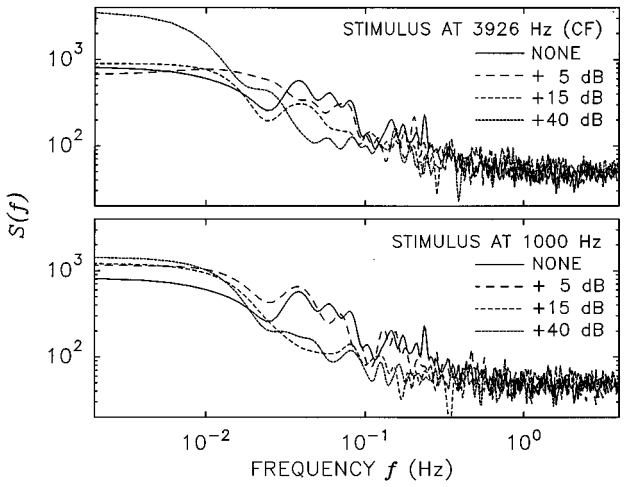

FIG. 5. Doubly logarithmic plots of the smoothed periodogram versus frequency for the same recordings as shown in Figs. 3 and 4 (neuron L-19). The periodogram is an estimate of the power spectral density of the spike train. The shapes of the curves resemble each other; all decrease approximately as power-law functions of the frequency, for sufficiently low frequencies. A larger estimated fractal exponent α_S is associated with driven firing.

$$A(T) \equiv \frac{\mathrm{E}\{[N(t+T,t+2T)-N(t,t+T)]^2\}}{2\mathrm{E}[N(t,t+T)]}. \tag{3}$$

It is related to the Fano factor by (Scharf *et al.*, 1995)

$$A(T) = 2F(T) - F(2T). \tag{4}$$

In general, both quantities vary with the counting time T. Indeed, for an FSPP with $0<\alpha<1$, the FF and the AF both vary as $\sim T^{\alpha}$, with the same fractal exponent α, over a large range of counting times T. Thus doubly logarithmic plots of the AF for such processes will yield an estimate α_A of the fractal exponent similar in value to α_F.

In contrast to the FF, however, the AF can rise as fast as $\sim T^3$ (see the Appendix). Thus it can be used to estimate fractal exponents over the expanded range $0<\alpha<3$. Figure 4 displays Allan factors for the same data sets used to obtain the FF plots shown in Fig. 3. For larger values of the counting time T, the AF curves all rise in approximately power-law fashion, much as the FF curves do, but with a larger onset time (Lowen and Ryu, 1996). Although a given AF generally appears visually rougher than its FF counterpart, it nevertheless generally provides a superior estimate of the fractal exponent (Teich *et al.*, 1996a). The Allan factor has been used successfully in connection with the sequence of human heartbeats, for which the values of α almost always exceed unity (Turcott and Teich, 1996).

For the spontaneous firings represented by the solid curves in Figs. 3 and 4, the slopes of the AFs closely resemble those of the corresponding FFs (see Table 1). This is expected, since the fractal exponent appears to be less than unity for spontaneous activity. However, for the driven recordings of this particular neuron, the AF slopes α_A exceed the corresponding FF slopes α_F in the long-time power-law regime, and in fact α_A sometimes exceeds unity.

The second measure with a power-law exponent not constrained to lie below unity is the periodogram (PG). It is denoted $S(f)$ and provides an estimate of the power spectral density of a point process. Much as for continuous-time processes, it reveals how the power is concentrated in various frequency bands. For an FSPP, the PG decreases as a power-law function of the frequency f so that $S(f) \sim f^{-\alpha_S}$ over a significant range of low frequencies (Lowen and Teich, 1995a). Nonfractal processes, in contrast, exhibit no such scaling over any significant range of frequencies. This fractal exponent α_S will assume a value similar to α_A obtained from the AF when $0<\alpha<3$, and to α_F obtained from the FF when $0<\alpha<1$. It appears that α_S does not saturate at *any* value, in contrast to α_F and α_A.

In Fig. 5 we present periodogram plots for the same data sets which provided the FFs shown in Fig. 3 and the AFs shown in Fig. 4. The periodograms all decrease in approximately power-law fashion for low frequencies, and reveal a larger fractal exponent α_S for the driven recordings than for spontaneous firing. This accords with similar observations of α_F and α_A. Examination of Table I reveals that whereas both α_S and α_A exceed unity for some recordings, α_F never does.

For an ideal FSPP, α_S, α_F, and α_A all coincide when they lie in the range $0<\alpha<1$, and $\alpha_S=\alpha_A$ for $0<\alpha<3$. In principle, any of these statistics may be obtained from a particular data set, but in practice each would yield a different number, thus giving rise to a family of fractal exponents. For a FSPP of sufficient duration, however, these three quantities will differ only slightly (within the ranges specified above), and furthermore will not depend significantly on the ranges of times and frequencies over which they are computed. In this case the point process under consideration may be said to be fractal, and α_S, α_A, and sometimes α_F, provide estimates of the true, underlying fractal exponent.

II. DATA ANALYSIS

The experimental data sets comprised spike trains from various cat primary auditory-nerve fibers, stimulated by a

variety of continuous-tone signals. The methods used for the collection of data were described previously (Delgutte, 1990; Kelly, 1994; Kelly *et al.*, 1996).

The data were processed as follows. The initial 100 s of each recording was discarded to ensure that stimulus-onset nonstationarities were not present. Data at the end of each recording were also discarded in those cases where the experimental notes indicated a problem, or where unphysiological changes were apparent. In recording L-16-3, for example, the number of counts in adjacent 1-s counting windows had a mean and standard deviation that were both less than unity, but for one such window near the end of the recording, eleven counts were registered; the data stretching from 5 s before that window to the end of the recording were discarded. Finally, all spikes occurring closer than 0.6 ms from the previous spike were discarded.

Since fractal fluctuations contain significant low-frequency components, relatively long data sets are required for proper analysis; as a result all recordings which did not exceed 100 s after implementing the previously described data selection procedures were discarded. We further discarded recordings for which the stimulus conditions were ambiguous, as well as those which exhibited unphysiological results (such as interevent intervals of 2000 s distributed throughout one data set).

No other processing was performed, with the goal of retaining all naturally occurring fractal behavior. Simulations of fractal processes reveal that FSPPs often contain segments which appear to be nonstationary, but which in fact are a legitimate part of the simulation. Eliminating these segments artificially reduces the amplitude of the fractal fluctuations in what is left of the recording, yielding a spuriously low estimate for the fractal exponent (Lowen and Teich, 1995a).

The net result was a total of 73 recordings, taken from 41 different neurons, that were suitable for study. These data were analyzed to obtain estimates of the fractal exponent using the three measures discussed above: FF, AF, and PG.

Obtaining the best estimates of the fractal exponents α_F, α_A, and α_S is facilitated by employing the largest range of times $[T_{\mathrm{MIN}},T_{\mathrm{MAX}}]$ or frequencies $[f_{\mathrm{MIN}},f_{\mathrm{MAX}}]$ for which scaling behavior exists. The FF and the AF both involve variances. To obtain reliable estimates of both the ordinary and Allan variances at a counting time T requires that the duration or length L of the recording be several times this counting time. We have found that $T_{\mathrm{MAX}}=L/10$ forms a practical upper limit for the counting time T; the number of samples is then always at least 10 (Lowen and Teich, 1995a). For small values of the lower limit T_{MIN}, the slope is underestimated (so that the estimate is biased) because the FF and AF assume values near unity at very small T, and therefore no longer follow a power-law form. Various methods can be employed to minimize this effect (Kelly, 1994; Kelly *et al.*, 1996); these will be considered further in a later publication. Large values of T_{MIN}, on the other hand, only leave a small range of counting times and therefore lead to a large variance in the estimated fractal exponent. Thus there exists a bias–variance tradeoff. For the data records analyzed here, $T_{\mathrm{MIN}}=L/100$ provided a good compromise (Lowen and Teich, 1995a). Recordings of shorter length L necessarily lead to an underestimation of the underlying fractal exponent using this method, although this bias appears to be an unavoidable artifact of shorter recordings (Woo, 1991). Obtaining a precise estimate of the fractal exponent often requires a surprisingly large amount of data (Lowen and Teich, 1995a).

We computed the estimate of the PG by fast Fourier transforming the number of counts in adjacent windows of length $L/4096$, and then forming the magnitude-square of this result. The periodogram plots in Fig. 5 were smoothed to provide a clearer visual indication of the underlying fractal behavior. In the actual process of estimation this smoothing was not performed since the least-squares method renders this unnecessary; furthermore, smoothing only confounds the estimated value α_S (Lowen and Teich, 1995a). The PG does not derive from a variance, so the smallest frequency available may be used: $f_{\mathrm{MIN}}=1/L$. For the maximum frequency a similar bias–variance tradeoff exists as for the FF and AF; we found that $f_{\mathrm{MAX}}=50/L$ gave the best results, although the upper cutoff does not influence the final result significantly (Lowen and Teich, 1995a).

III. RESULTS AND DISCUSSION

For the 73 recordings studied, the estimates of the fractal exponent employing the FF (α_F), AF (α_A), and PG (α_S) were found to be in reasonably good agreement with each other, with an average rms difference of 0.24. This compares favorably with results from simulations of much longer data sets (10^6 points), in which accuracies of ± 0.1 were obtained (Lowen and Teich, 1995a). Some differences among the estimators are to be expected, since they derive from different statistical measures, and the relevant time and frequency ranges also differ. As expected, the FF-based estimator of α remained below unity for all 73 recordings. Figure 6 presents values of α_A and α_S for the 41 spontaneous records (open circles) and the 32 driven records (filled circles).

Generally, the estimated fractal exponents increased under stimulation in comparison with spontaneously firing conditions. This increase appears to be relatively independent of the characteristic frequency and spontaneous firing rate of the neuron, and on the nature and frequency of the stimulus (Woo, 1991). The only exceptions were two neurons which exhibited a small decrease in one of the estimators (α_F for L-19 decreased by 0.05 for a stimulus of +5 dB at CF, and α_A for R-12 decreased by 0.13 for a stimulus of +15 dB at CF), and one neuron (L-18) in which the estimated fractal exponent decreased an average of 0.40 for the three measures for a stimulus of +15 dB at CF. But for all other neurons, the estimated values of α increased under stimulation. Indeed, for the spontaneous data we found that $\alpha_A \leqslant 1.03$ and $\alpha_S \leqslant 1.09$ for all neurons, and for no neuron were both $\alpha_A \geqslant 1$ and $\alpha_S \geqslant 1$; we conclude that the true value of the fractal exponent α remains below unity under spontaneously firing conditions.

Four of the 32 data sets recorded with auditory stimulation appear to have fractal exponents with a true value greater than unity, since both the AF- and PG-based estimates exceed unity for these data files. These recordings are presented in Table I, together with all of the other recordings made from the same neurons. Both α_A and α_S are subject to

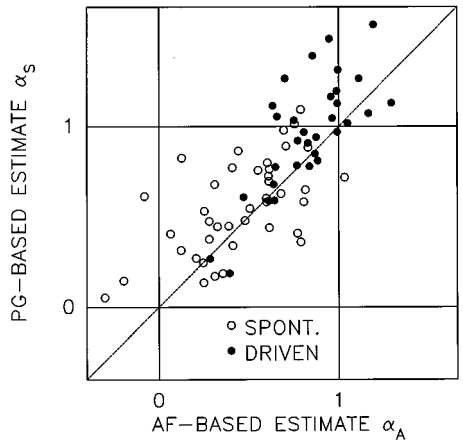

FIG. 6. Scatterplot of the estimated values of the fractal exponent for all 73 data sets. The Allan factor (AF) was calculated for each data set with the counting time ranging from $L/100$ to $L/10$ in ten logarithmically spaced steps, where L is the duration of the recording. The periodogram (PG) was calculated for frequencies ranging from $1/L$ to $50/L$ in 50 linearly spaced steps. The slope of a least-squares straight-line fit to a doubly logarithmic plot of the AF forms the abscissa, while the slope of a similar fit to the PG forms the ordinate. Spontaneously firing recordings are represented by open circles, and driven recordings by filled circles. Driven recordings generally deliver higher estimates of the fractal exponent than spontaneous recordings. The diagonal dotted line indicates where the two estimates would coincide. An infinite-length data set would yield a certain estimate for the fractal exponent; finite data sets yield estimates which themselves fluctuate about this value. Three of the resulting estimates for spontaneous data sets turn out to be negative as a result of these fluctuations.

variance arising from the finiteness of the data set, so that some of the variation in the estimated values of α among the different recordings stems from this estimation error. However, the correlation coefficient between the AF- and PG-based estimators of the fractal exponent assumes a value of $+0.760$ for the data sets recorded with a stimulus present, indicating that the log-log slopes of the AF and PG indeed estimate essentially the same underlying value, and do not merely represent random error in the estimation process. Confidence in these estimators also stems from the observation that the behavior of the spontaneously firing recordings on the whole differs from that of the driven data sets (see Fig. 6). Finally, simulations of FSPPs consistently show a bias away from unity, and toward lower values, for larger values of the intended fractal exponent (Lowen and Teich, 1995a; Teich *et al.*, 1996a). Thus if any bias exists we would expect α_A and α_S to underestimate the true underlying value α of the fractal exponent.

IV. CONCLUSION

Auditory-nerve spike trains exhibit fractal behavior. Such behavior is characteristic of long-term memory and reflects neuronal facilitation (see Baudry and Lynch, 1993). It has also been observed in sequences of action potentials in the cat visual system (Teich *et al.*, 1996a, 1996b, 1996c). In addition to rate fluctuations which persist over long averaging times, three measures indicate fractal activity: the Fano factor (FF); the Allan factor (AF), which we define; and the periodogram (PG). These three measures yield numerical estimates of the fractal exponent α, a number which is a characteristic of the spike-train data. Estimates of α based on the FF saturate at unity, but not so for those based on the AF and PG. In fact, these latter measures show that some stimulated recordings have a fractal exponent α in excess of unity. Generalized versions of the FF and AF, based on various families of wavelet functions, provide additional means for estimating the fractal exponent of a sequence of nerve spikes (Flandrin and Abry, 1992; Teich *et al.*, 1996a; Heneghan *et al.*, 1995; Abry and Flandrin, 1996). Finally, we mention that analytical techniques which incorporate the effects of refractoriness into fractal models of neural spike trains yield robust estimates of fractal exponents (Lowen and Teich, 1995b).

ACKNOWLEDGMENTS

The authors are grateful to B. Delgutte and D. H. Johnson for graciously sharing their data. This work was supported by the Whitaker Foundation under Grant No. CU01455801 and by the Office of Naval Research under Grant No. N00014-92-J-1251.

APPENDIX: MAXIMUM POWER-LAW EXPONENT OF THE ALLAN FACTOR

The Allan factor for a data set may rise no faster than T^3 as a function of the counting time T over significant ranges of T. With $N(s,t)$, as before, denoting the number of events counted in a counting window starting at time s and ending at time t, we reiterate the definition of the Allan factor given in Eq. (3):

$$A(T) \equiv \frac{\mathrm{E}\{[N(T,2T)-N(0,T)]^2\}}{2\mathrm{E}[N(0,T)]}, \tag{A1}$$

where we have simplified the notation by setting the arbitrary starting time to $t=0$. For a counting time twice as large we obtain

$$\begin{aligned} A(2T) &= \mathrm{E}\{[N(2T,4T)-N(0,2T)]^2\}/2\mathrm{E}[N(0,2T)] \\ 2\mathrm{E}[N(0,2T)]A(2T) &= \mathrm{E}\{[N(3T,4T)+N(2T,3T) \\ &\quad -N(T,2T)-N(0,T)]^2\} \\ 4\mathrm{E}[N(0,T)]A(2T) &= \mathrm{E}[\{[N(3T,4T)-N(2T,3T)]+2[N(2T,3T) \\ &\quad -N(T,2T)]+[N(T,2T)-N(0,T)]\}^2] \\ &\leqslant \mathrm{E}[\{4[N(T,2T)-N(0,T)]\}^2] \\ &= 32\mathrm{E}[N(0,T)]A(T). \end{aligned} \tag{A2}$$

Therefore $A(2T) \leqslant 2^3 A(T)$. A similar approach yields $A(nT) \leqslant n^3 A(T)$ for any arbitrary positive integer n. Thus over large ranges of counting times T, the Allan factor can increase no faster than $\sim T^3$.

Many stochastic point processes achieve this upper limit of $\sim T^3$; we illustrate that this limit can be achieved with a simple process whose rate $\lambda(t)$ varies sinusoidally:

$$\lambda(t) = \lambda_0[1+\cos(\omega t+\phi)], \tag{A3}$$

where λ_0 and ω are parameters and ϕ is a random variable uniformly distributed over $[0,2\pi]$. We focus on the counting-time limits $\lambda_0^{-1} \ll T \ll \omega^{-1}$, where the discrete events are well represented by a continuous rate function. The number of events in a counting window $(0,T)$ then becomes

$$\begin{aligned} N(0,T) &= \int_0^T \lambda(u)\,du \\ &= \lambda_0 T + \lambda_0 \omega^{-1}[\sin(\omega T+\phi)-\sin(\phi)] \\ &= \lambda_0 T + 2\lambda_0 \omega^{-1} \sin(\omega T/2)\cos(\omega T/2+\phi). \end{aligned} \tag{A4}$$

The expected number of events is simply $\mathrm{E}[N(0,T)] = \lambda_0 T$, while the variance is given by

$$\begin{aligned} \mathrm{Var}[N(0,T)] &= 4\lambda_0^2 \omega^{-2} \sin^2(\omega T/2)\mathrm{E}[\cos^2(\omega T/2+\phi)] \\ &= 2\lambda_0^2 \omega^{-2} \sin^2(\omega T/2) \\ &\approx 2\lambda_0^2 \omega^{-2}[(\omega T/2)^2 - 3^{-1}(\omega T/2)^4] \\ &= 2^{-1}\lambda_0^2 T^2 - 24^{-1}\lambda_0^2 \omega^2 T^4, \end{aligned} \tag{A5}$$

where the condition $\omega T \ll 1$ permits the use of a power-series expansion for the sine function. Dividing the variance by the mean yields the Fano factor

$$F(T) \approx 2^{-1}\lambda_0 T - 24^{-1}\lambda_0 \omega^2 T^3, \tag{A6}$$

which, when substituted into Eq. (3), yields

$$A(T) = 2F(T) - F(2T) \approx 4^{-1}\lambda_0 \omega^2 T^3 \tag{A7}$$

to first order in T.

Abry, P., and Flandrin, P. (**1996**). ''Point processes, long-range dependence, and wavelets,'' in *Wavelets in Medicine and Biology*, edited by A. Aldroubi and M. Unser (CRC, Boca Raton, FL), pp. 413–437.

Allan, D. W. (**1966**). ''Statistics of atomic frequency standards,'' Proc. IEEE **54**, 221–230.

Barnes, J. A., and Allan, D. W. (**1966**). ''A statistical model of flicker noise,'' Proc. IEEE **54**, 176–178.

Baudry, M., and Lynch, G. (**1993**). ''Long-term potentiation: biochemical mechanisms,'' in *Synaptic Plasticity: Molecular, Cellular, and Functional Aspects*, edited by M. Baudry, R. F. Thompson, and J. L. Davis (MIT, Cambridge, MA), pp. 87–115.

Delgutte, B. (**1990**). ''Physiological mechanisms of psychophysical masking: Observations from auditory nerve fibers,'' J. Acoust. Soc. Am. **87**, 791–809.

Flandrin, P., and Abry, P. (**1992**). ''Time-scale analyses and self-similar stochastic processes,'' Proc. NATO Advanced Study Institute on Wavelets and their Applications (Il Ciocco, Italy).

Gaumond, R. P. (**1993**). ''Ratio of variance to mean of action potential counts for an auditory nerve fiber model with second-order refractory behavior,'' J. Acoust. Soc. Am. **93**, 2035–2037.

Gaumond, R. P., Molnar, C. E., and Kim, D. O. (**1982**). ''Stimulus and recovery dependence of cat cochlear nerve fiber spike discharge probability,'' J. Neurophysiol. **48**, 856–873.

Heneghan, C., Lowen, S. B., and Teich, M. C. (**1995**). ''Wavelet analysis for estimating the fractal properties of neural firing patterns,'' Proc. Fourth Ann. Comp. Neurosci. Meeting (Monterey, CA).

Kelly, O. E. (**1994**). ''Analysis of long-range dependence in auditory-nerve fiber recordings,'' Master's thesis, Rice University.

Kelly, O. E., Johnson, D. H., Delgutte, B., and Cariani, P. (**1996**). ''Fractal noise strength in auditory-nerve fiber recordings,'' J. Acoust. Soc. Am. **99**, 2210–2220.

Kumar, A. R., and Johnson, D. H. (**1993**). ''Analyzing and modeling fractal intensity point processes,'' J. Acoust. Soc. Am. **93**, 3365–3373.

Li, J., and Young, E. D. (**1993**). ''Discharge-rate dependence of refractory behavior of cat auditory-nerve fibers,'' Hear. Res. **69**, 151–162.

Lowen, S. B., and Ryu, B. K. (**1996**). In preparation.

Lowen, S. B., and Teich, M. C. (**1992**). ''Auditory-nerve action potentials form a nonrenewal point process over short as well as long time scales,'' J. Acoust. Soc. Am. **92**, 803–806.

Lowen, S. B., and Teich, M. C. (**1993**). ''Estimating the dimension of a fractal point process,'' Proc. SPIE **2036**, 64–76.

Lowen, S. B., and Teich, M. C. (**1995a**). ''Estimation and simulation of fractal stochastic point processes,'' Fractals **3**, 183–210.

Lowen, S. B., and Teich, M. C. (**1995b**). ''Refractoriness-modified fractal stochastic point processes for modeling sensory-system spike trains,'' Proc. Fourth Ann. Comp. Neurosci. Meeting (Monterey, CA).

Powers, N. L., and Salvi, R. J. (**1992**). ''Comparison of discharge rate fluctuations in the auditory nerve of chickens and chinchillas,'' in *Abstracts of the Fifteenth Midwinter Research Meeting of the Association for Research in Otolaryngology*, edited by D. J. Lim (Association for Research in Otolaryngology, Des Moines, IA), Abstract 292, p. 101.

Powers, N. L., Salvi, R. J., and Saunders, S. S. (**1991**). ''Discharge rate fluctuations in the auditory nerve of the chinchilla,'' in *Abstracts of the Fourteenth Midwinter Research Meeting of the Association for Research in Otolaryngology*, edited by D. J. Lim (Association for Research in Otolaryngology, Des Moines, IA). Abstract 411, p. 129.

Ricciardi, L. M., and Esposito, F. (**1966**). ''On some distribution functions for non-linear switching elements with finite dead time,'' Kybernetik (Biol. Cybern.) **3**, 148–152.

Scharf, R., Meesmann, M., Boese, J., Chialvo, D. R., and Kniffki, K. (**1995**). ''General relation between variance-time curve and power spectral density for point processes exhibiting $1/f^{\beta}$-fluctuations, with special reference to heart rate variability,'' Biol. Cybern. **73**, 255–263.

Teich, M. C. (**1989**). ''Fractal character of the auditory neural spike train,'' IEEE Trans. Biomed. Eng. **36**, 150–160.

Teich, M. C. (**1992**). ''Fractal neuronal firing patterns,'' in *Single Neuron Computation*, edited by T. McKenna, J. Davis, and S. Zornetzer (Academic, Boston), pp. 589–625.

Teich, M. C., and Lowen, S. B. (**1994**). ''Fractal patterns in auditory nerve-spike trains,'' IEEE Eng. Med. Biol. Mag. **13**, 197–202.

Teich, M. C., Matin, L., and Cantor, B. I. (**1978**). ''Refractoriness in the maintained discharge of the cat's retinal ganglion cell,'' J. Opt. Soc. Am. **68**, 386–402.

Teich, M. C., Johnson, D. H., Kumar, A. R., and Turcott, R. G. (**1990a**). ''Rate fluctuations and fractional power-law noise recorded from cells in the lower auditory pathway of the cat,'' Hear. Res. **46**, 41–52.

Teich, M. C., Turcott, R. G., and Lowen, S. B. (**1990b**). ''The fractal doubly stochastic Poisson point process as a model for the cochlear neural spike train,'' in *The Mechanics and Biophysics of Hearing (Lecture Notes in Biomathematics, Vol. 87)*, edited by P. Dallos, C. D. Geisler, J. W. Matthews, M. A. Ruggero, and C. R. Steele (Springer-Verlag, New York), pp. 354–361.

Teich, M. C., Heneghan, C., Lowen, S. B., and Turcott, R. G. (**1996a**). ''Estimating the fractal exponent of point processes in biological systems using wavelet- and Fourier-transform methods,'' in *Wavelets in Medicine and Biology*, edited by A. Aldroubi and M. Unser (CRC, Boca Raton, FL), pp. 383–412.

Teich, M. C., Turcott, R. G., and Siegel, R. M. (**1996b**). ''Variability and long-duration correlation in the sequence of action potentials in cat striate-cortex neurons,'' IEEE Eng. Med. Biol. Mag. (to be published).

Teich, M. C., Heneghan, C., Lowen, S. B., Ozaki, T., and Kaplan, E. (**1996c**). ''Fractal character of the neural spike train in the visual system of the cat,'' J. Opt. Soc. Am. A (submitted).

Turcott, R. G., and Teich, M. C. (**1996**). ''Fractal character of the electrocardiogram: Distinguishing heart-failure and normal patients,'' Ann. Biomed. Eng. **24**, 269–293.

Young, E. D., and Barta, P. E. (**1986**). ''Rate responses of auditory nerve fibers to tones in noise near masked threshold,'' J. Acoust. Soc. Am. **79**, 426–442.

Woo, T. W. (**1991**). ''Fractals in auditory-nerve spike trains,'' Master's thesis, Johns Hopkins University, Baltimore.

Woo, T. W., Sachs, M. B., and Teich, M. C. (**1992**). ''$1/f$-like spectra in cochlear neural spike trains,'' in *Abstracts of the Fifteenth Midwinter Research Meeting of the Association for Research in Otolaryngology*, edited by D. J. Lim (Association for Research in Otolaryngology, Des Moines, IA), Abstract 295, p. 101.